Süleyman Demirel Üniversitesi
Fen Bilimleri Enstitüsü Dergisi
Cilt 21, Sayı 3, 673-682, 2017

Süleyman Demirel University
Journal of Natural and Applied Sciences
Volume 21, Issue 3, 673-682, 2017

DOI: 10.19113/sdufbed.38730

The Effect of Welding Parameters on Microstructural and Mechanical Properties of HSLA S960QL Type Steel with Submerged Arc Welding

Mehmet TÜRKER[*1]

[1]University of National Defense, Department of Mechanical Engineering, 34940, İstanbul

(Alınış / Received: 12.04.2017, Kabul / Accepted: 02.06.2017, Online Yayınlanma / Published Online: 08.08.2017)

Keywords
HSLA,
Submerged arc welding,
Microstructural and mechanical properties

Abstract: In this study, S960QL steels were welded with submerged arc welding process in order to examine microstructural and mechanical properties. For the microstructural investigation, microscopical examination methods were used for weld zones. Tensile, impact toughness and micro hardness tests were made for different samples obtained from the weld zone and the base metal. The examinations of fracture surfaces were made by using optical microscope and scanning electron microscope. The flat type tensile strength values were near to the base materials. Charpy impact toughness tests were made for the base metal, the weld metal center line, the fusion line, the zone between weld metal centerline and the fusion line. Impact energy of the weld metal was obtained lower than the base metal. The lowest impact energy was obtained at the fusion line. Heat affected zone had the highest value in micro hardness tests. In microstructure evaluation, the interface of the fusion zone-heat affected zone and heat affected zone had coarser grain structure than the base metal. Alloy carbides dissolved because of the high temperature values occurred at heat affected zone.

Tozaltı Ark Kaynağı Yöntemi Birleştirilen HSLA S960QL Çeliğinde Kaynak Parametrelerinin Mikroyapı ve Mekanik Özellikler Üzerinde Etkisi

Anahtar Kelimeler
HSLA,
Tozaltı ark kaynağı,
Mikroyapısal ve mekanik özellikler

Özet: Bu çalışmada; S960QL düşük karbonlu ve yüksek mukavemetli düşük alaşımlı çelikler, mikroyapı ve mekanik özelliklerinin araştırılması amacıyla tozaltı ark kaynağı yöntemi kullanılarak kaynak edilmişlerdir. Mikroyapısal incelemelerde tozaltı kaynak bölgeleri için mikroskobik muayene teknikleri uygulanmıştır. Kaynak ve ana metalden elde edilen farklı numunelerin mekanik özellikleri için çekme, darbe ve mikro sertlik testleri yapılmıştır. Yassı çekme numune mukavemet değerleri ana metale yakın değerler vermiştir. Fakat kaynak metalinden elde edilen yuvarlak tip çekme numune dayanımları ana metalden çok düşük çıkmıştır. Kopan parçaların kırılma yüzeyleri optik ve taramalı elektron mikroskobu ile incelenmiştir. Charpy darbe testleri; ana metal, kaynak metali merkez hattı, ergime hattı, kaynak metali merkez hattı ve ergime hattı arası bölgelerinden yapılmıştır. Kaynak metali ergime hattı darbe enerjisi ana metalden daha düşük ölçülmüştür. En düşük darbe enerjisi ergime hattında ölçülmüştür. Mikrosertlik testlerinde, en yüksek değer ısıdan etkilenmiş bölgeden ölçülmüştür. Mikroyapı analizlerinde, kaynak dikişi-ısıdan etkilenmiş bölge ara yüzeyi ve ısıdan etkilenmiş bölge mikroyapılarının ana malzemeye göre daha büyük taneli olduğu görülmüştür. Isıdan etkilenmiş bölge ortaya çıkan yüksek sıcaklık değerleri nedeniyle alaşım karbürleri çözünmüş ve tane büyümesi daha kolay bir şekilde gerçekleşmiştir.

1. Introduction

High-strength, low-alloy (HSLA) steels constitute a successful metallurgical innovation in which alloying additions and thermomechanical processing have been brought together effectively to attain improved combinations (high tensile strength with good notch toughness, ductility, corrosion resistance, adequate formability or weldability than convention carbon steel in the normal sense) of engineering properties

*Corresponding author: mehmetturker75@gmail.com

through microstructural control. The physical metallurgy principles in HSLA steels include inclusion morphology, carbonitride solubility, grain refinement, precipitation hardening and substructure strengthening. While substantial improvements have been made in the thermomechanical processing of steels, the secret of the success of HSLA steels is in the micro alloying where the addition of small amounts of elements such as niobium, titanium or vanadium can make all the difference. They are designed to meet specific mechanical properties rather than a chemical composition [1-13].

Exceptional combination of these advantages is a crucial need for thick steel plates used for the manufacturing of pressure vessels, ship hulls, line pipes, automobile, earth moving, mining equipment and various other strategic defense applications [9-18].

In HSLA steels, carbonitrides, nitrides and micro alloy carbides are critical in order to control the austenite recrystallization and grain growth during steelmaking and welding, causing the acceptable grain refining. Also, microalloyed rolling and rapid cooling cause to form non-polygonal or acicular ferrite and bainite which make further contribution to strengthen [19]. Particularly, titanium is added to these steels for controlling of the austenite grain size in the course of welding or reheating process [20, 21].

It is crucial to recognize the microstructures of the weld zone in order to predict the strength and toughness of the welded joint. Although these steels have fine-grained microstructure and favorable properties, the toughness can be failed during welding because of microstructural changes in heat-affected zone (HAZ). The coarse-grained HAZ (CGHAZ) generally has the lowest toughness among the different zones inside HAZ due to its unsuitable microstructure. During welding process, the CGHAZ is subjected to high temperature near the melting point and rapid cooling. This high temperature causes the remarkable austenite grain growth and following fast cooling supports slightly brittle microstructures in this zone. Besides the thermal cycle, the CGHAZ is exposed to thermal stress and strain because of constraint by the thermally unaffected parent metal during welding. Because of that, welded joint of HSLA is the weakest part of the whole welded structure under fatigue conditions [22-23].

S960QL steels in low carbon-low alloy group are very common in the heavy transport, mining and lifting industry, where mobile or fixed structures have to carry high loads – often in safety critical situations. In order to sustain their extreme characteristics, it is must to know or predict the mechanical properties according to the chosen parameters defined in the standards.

In this experimental investigation and relevant analyses, the influence of parameters was studied according to the ISO 26304:2011 classification. In order to determine these parameters; the current, voltage and wire speed between the applicable ranges were tried in the welding laboratory, and then according to the penetration and visual tests the acceptable welding parameters were selected. Thus, the microstructural and mechanical properties of submerged arc welding (SAW) welds of 25 mm thick S960QL HSLA steel according to the selected parameters were found out, instead of comparing the different welded samples.

2. Material and Method

S960QL steels were welded by using submerged arc welding process. For the microstructural investigation, microscopical examination methods were used in weld zones. Different samples obtained from the weld metal and the base metal, were subjected to tensile, impact toughness and micro hardness tests. Fracture surfaces were examined by optical microscope and scanning electron microscope. Charpy impact toughness tests were made for the base metal, the weld metal center line (WMCL), the fusion line (FL), the zone between WMCL and FL.

2.1. Material

S960QL (1.8933) steel was used as the sample material. It was supplied as hot rolled flat nominally 25 mm diameter. Metal sheets were cut to lengths suitable for SAW. The chemical composition and mechanical properties of the base metal is given in Table 1. They were obtained by the optical emission spectrometry and producer, respectively.

Table 1. Chemical composition and mechanical properties of the base material. (wt-%)

C	**Si**	**Mn**	**P**	**S**	**Al**	**N**	**Cu**
0.18	0.29	0.89	0.010	0.001	0.043	0.04	0.015
Mo	**Ni**	**Cr**	**V**	**Nb**	**Ti**	**B**	**Ca**
0.52	1.00	0.47	0.04	0.01	0.001	0.0002	0.0015
Tensile strength (MPa)			**Minimum yield strength (MPa)**			**Elongation (%)**	
980-1150			960			10	

2.2. Welding

The SAW process was realized automatically in the laboratory setting for chemical, hardness and microstructural investigations by using single and multilayer welding. Chemical oxide removal processes were applied prior to and before welding all samples were cleaned from all contaminations by using acetone and stainless steel brush. Table 2 presents the chemical analysis of the applied 4 mm diameter filler wire. The flux (EN ISO 14174) is an agglomerated fluoride-basic flux with high basicity and neutral metallurgical behavior. It is suitable for single (AC or DC). The welding machine is ESAB Aristo 1000.

Table 2. Filler wire specified composition values.

Filler Wire	C	Si	Mn	P	S	Cr	Ni	Mo
EN ISO 26304-A SZ3Ni2,5CrMo AWS A5.23	0.14	0.10	1.75	≥0.012	≥0.012	0.35	2.10	0.60

In the light of information obtained from literature review and preliminary tests, chemical, hardness and microstructural experiments were carried out by using the parameters as follows: multiple weld beads were made on the base metal with a thickness of 25 mm with weld groove as shown in Figure 1. The welding seams were made transverse to rolling direction of the base material as PA welding position.

In order to determine welding parameters according to EN ISO 26304:2011, the values between the range of 450-550 A, 25-35 V and 85-95 mm/min wire speed for 4 mm wire diameter were tried in the welding laboratory and then according to the penetration and visual tests, the appropriate welding parameters were selected. No preheat was applied. The welding details of the joints are given in Table 3.

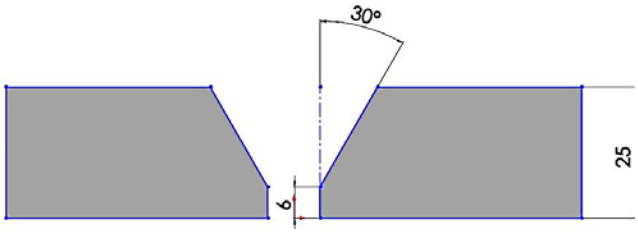

Figure 1. Dimensions for the V-groove weld.

Table 3. SAW parameters for mechanical, hardness and microstructural investigations.

Wire diameter (mm)	Wire speed (mm/min)	Voltage (V)	Current (A)	Welding speed (m/min)
4.0	93	29	~525	0.5

2.3. Chemical analyses

Single layer weld metal was investigated in order to compare its chemical analysis with the base metal. The chemical analyze of the single layer weld metal was made from the point as shown in Figure 2. The measurements were done at least three times by the optical emission spectrometry-Specrolab/Spectro Analythical Instruments Gmbh.

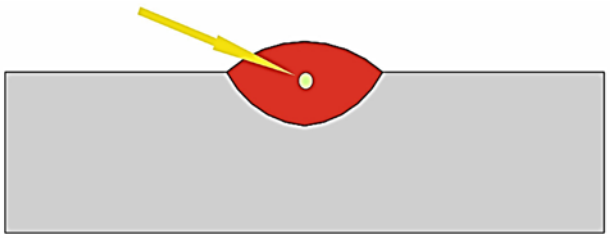

Figure 2. The chemical analysis point of single layer weld metals.

2.4. Microstructural investigation

Submerged arc welded joints of S960QL were cross-sectioned perpendicular to the welding direction. In the first step, specimens were prepared with standard metallographic preparations like grinding, polishing and etching with %3 nital for 10–15 seconds at room temperature. In the second step, the weld zones were visualized as macrographs and investigated as micrographs by LOM with magnifications of 50X, 200X and 500X.

2.5. Hardness

As an additional destructive test method, Vickers micro hardness measurement (HV 0.3) was carried out under a load of 2.942 N over cross sections on vertical (the welding centerline) and horizontal lines 1 mm distance between each indentation on metallographic specimen taken from each welded plate with Shimadzu HMV-2000. EN ISO 6507-1:2005 test method was applied on the single layer and multiple layer welded sample.

2.6. Tensile test

The transverse tensile test specimens were taken and prepared from the welded plates, transverse and longitudinal to the weld seam with reference to DIN 50125 Form B and E. The notation of transverse sample and longitudinal is DIN 50125 – A 10 x 50 and DIN 50125 – E 8 x 25 x 80 respectively. The tests were made by using a hydraulically controlled test machine (Instron 600 kN) with a 600-kN capacity at room temperature in accordance to European Standard (DIN EN ISO 6892-1). The transverse tensile test specimens were extracted from top, middle and bottom part of the welded joint as flat type (Figure. 3).

2.7. Notch impact toughness test

Four different samples were extracted transverse to the weld and notched WMCL (1), the zone between WMCL and FL (2), FL (3) and the base metal (4), as shown in Figure 4. The tests were performed in

accordance with EN 10045-1 and DIN EN ISO 9016 at the room temperature.

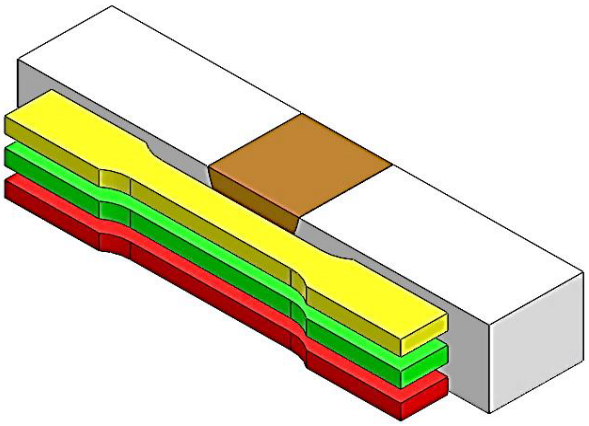

Figure 3. Schematic illustration of flat tensile test samples.

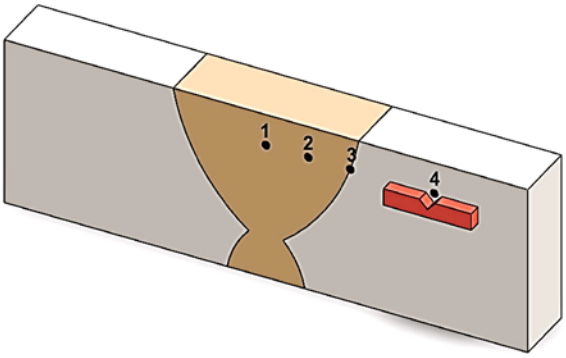

Figure 4. Schematic illustration of the test points of the notch impact toughness test samples.

3. Results

3.1. Chemical analyses

Investigating the chemical analyses results, the mean values were obtained between the weld metal and the filler wire compositions. The effect of experimental parameter changing on the distribution of alloying elements was not occurred since the analyses were carried out from the wide zone. Chemical composition of the weld deposit of single layer weld metal is presented in Table 4.

Table 4. The chemical composition of single layer weld metal used 4 mm wire diameter. (wt-%)

C	Si	Mn	P	S	Cr	Mo	Ni	Al	Co
0.123	0.312	1.15	0.0079	<0.001	0.408	0.525	1.35	0.0249	0.0077
Cu	**Nb**	**Ti**	**V**	**W**	**Pb**	**Sn**	**As**	**Zr**	**Ca**
0.0291	0.0057	0.0013	0.0318	0.0096	<0.001	0.0017	0.0025	0.0017	<0.0005
Ce	**Sb**	**Se**	**Te**	**Ta**	**B**	**Zn**	**Bi**	**Fe**	
0.0039	<0.0003	0.0062	<0.005	0.0036	<0.0005	0.0033	0.0038	95.8	

3.2. Hardness

The hardness assessment was made on metallography specimens for single layer and multiple layer, in order to present results from the point of heat input effect on hardness.

In single layer measuring, as shown in Figure 5, maximum base metal hardness ranged from 316 HV0.3 to 357 HV0.3. Weld metal hardness of the welds varied between 300 and 340 HV0.3. Maximum hardness values 410-430 HV0.3 were measured at the HAZ on both vertical and horizontal rows. The base metal has an oriented structure. Also the excessive heat caused recrystallization. These high hardness values are owing to this occurring of recrystallization condition and cooling rate. Hardness values of the weld seam center region are close to the base metal. Examining the values from the weld seam to the base metal, they decreased at the weld seam-HAZ interface. The grain growth observed in this zone was due to the heat transfer from the weld seam through to the base metal. Because of that, the grain coarsening occurred at the weld seam-HAZ interface significantly and the hardness values decreased.

The welded sample has massive martensite in HAZ adjacent to the weld metal, based on high heat input and cooling conditions. The decreasing of micro hardness due to the grain coarsening was eliminated with martensite occurring. At the vertical line to the weld center, the lower hardness values were determined.

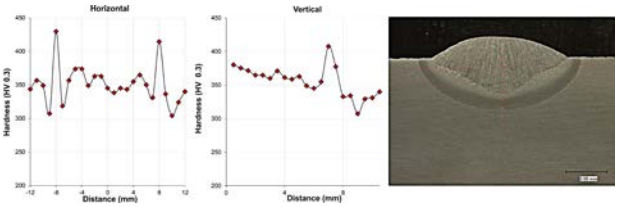

Figure 5. The microhardness results of single layer weld metal sample.

Figure 6 shows the hardness distributions of welded specimen for multilayer welding. The fusion zone (FZ) and HAZ were subjected to the phase transformations. This caused that the hardness values on the weld zone and the base metal changes considerably. Weld metal hardness of the welds varied between 275 and 315 HV0.3 (Figure 6a). Maximum hardness values were measured as 395-410 HV0.3 at the HAZ. The FZ values were close to the base metal. The intersection of the root pass and the WMCL revealed 340-380 HV0.3 values. At the row of the root pass from the center line to base metal, HAZ zone exhibited 350-448 HV0.3. Such hardness values for both multilayer passes and root pass reveal the potential risk of cracks in HAZ. This is an indicator that the HAZ structure contains micro-structural constituents which are susceptible to the occurrence of cold cracks. Moreover, the root FZ hardness had higher than the weld metal (311-347 HV0.3).

Comparing single layer welding hardness with the multi-layer, the reheating of each subsequent weld pass normalized and refined the microstructure in the former weld pass during the welding thermal cycle. After each weld run, the previous weld metal was tempered and the residual stresses were

minimized. Thus, the preheating was provided and the cooling rate of weld joint was decelerated. These reasons can have an impact on different hardness values, even a little.

The grain size is a parameter which directly affects the mechanical properties of metals and alloys. In fine grained materials, mechanical properties are high due to increase of grain boundary. During the welding process, high temperature values in HAZ are observed because of the high heat input. The grain coarsening is seen in the microstructure and also the mechanical properties decrease. At the same time, the alloying elements in the structure of these steels form finely dispersed carbides. The dissolution of alloy carbides takes place on account of the high heat input effect during welding. It causes a reduction in mechanical properties. Additionally, because of the carbide dissolution, grain boundaries are released and grain growth during welding becomes easier. It is seen that the micro hardness results are compatible with the literature [25,26].

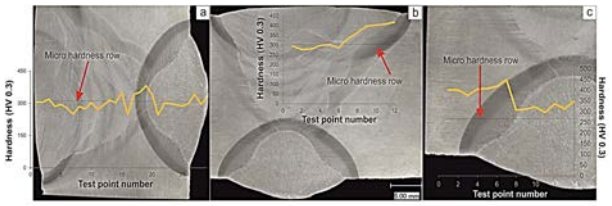

Figure 6. The graphical presentation of micro hardness results of; a) the weld centerline, b) the row from the weld centerline to HAZ, c) the root pass from the center line to the base metal.

3.3. Tensile test

Investigating the tensile test specimens, fractures occurred outside of the welded joint. Taking account of SAW, a high heat input occurs according to the other welding processes. A high heat input promotes grain growth and this has an adverse effect on both strength and toughness. At the same time, it causes decreasing the material hardness. Since both hardness and tensile strength present the resistance against the plastic deformation of metals, two data are directly proportionate roughly. In other saying, fracture occurring outside of the base metal which has almost similar hardness values with the weld metal verifies the result. The tensile strength of flat type samples (N-MPa), minimum yield strength (N-MPa), elongation (%) values expressed are presented in Table 5.

Table 5. The tensile test results (average values).

Type	Tensile strength (MPa)	Minimum yield strength (MPa)	Elongation (%)
Flat (top)	918.1	824.3	8.91
Flat (middle)	1018.65	960.71	8.85
Flat (bottom)	1023.3	971.65	8.74

Analyzing the tensile strength results of the welded joints, the middle and the bottom flat type samples exhibited higher values than the base metal values (>980 MPa) obtained by the producer and literature. The top flat type samples were relatively lower than the other flat samples. These samples have the wider weld metal. On the other hand, it is clear that the welded samples are not homogenous. Due to these reasons, it is evaluated as normal. The elongations of the flat type samples were lower than the base metal. The hardness results revealed that the weld zone hardness decreased by the welding process. This is presumably to explain the lower elongation. Due to the fact that the weld zone had lower hardness than base metal, deformation occurred adjacent to this zone. At the same time, occurring of the deformation in narrow area resulted in decreasing of the elongation. Previous studies supported this [27,28]. In conclusion, the resistance of the FZ and HAZ against the deformation caused that the elongation values of the flat type samples decreased.

The fractured surfaces of the tensile samples were investigated by LOM and SEM. Fig. 10(a), (b) and (c) show them. The modes of failure of the tensile test samples were ductile with acceptable plastic deformation and are evident from the fracture location and fractured surface shown in the figures. Despite the fracture type being ductile, the lower elongation values of the welded samples should not be seen as a contradiction. Fine and secondary dimples are signs of good tensile strength of this joint. If the dimple sizes are finer, the strength and ductility of the joints are higher.

3.4. Notch impact toughness test

In order to compare four different zones, 55mm × 10mm × 10mm test pieces were used. The tests were carried out at room temperature (~21°C). The notch impact values pointed out in joule are presented in Figure 9.

The base material gave the highest toughness values, 185 J, 177.5 J, and 173 J. These results are almost compatible with Reference 27. The specimens between WMCL and FL achieved the best absorbed energies between 136.5 and 140.5 Joule, following the base metal. The impact energy values for FL varied from 96 to 104 Joule. The toughness of HAZ coarsened grain zone in HAZ was more than weld metal. In a study on fracture behaviors of welded low carbon steels [29], the similar result was obtained. Comparing with the base metal, the impact values of WMCL, FL and between WMCL and FL are lower. The application of welding parameters affected impact toughness of S960QL steel. The impact toughness tests which are carried out in the room temperature were lower according to base metal. These steels are specially produced with high tensile strength and toughness. However, it is normal that the tensile strength and the toughness had low values, due to the

deterioration of the grain structure, grain refining elements forming precipitates in the form of carbide and carbonitride and changing the types and shapes of the precipitates with the effect of heat input. In addition; due to the fact that the structure produced as homogeneous lost this homogeneity relatively with the heat input effect, the coarsed grain structure having low toughness is one of the expected results.

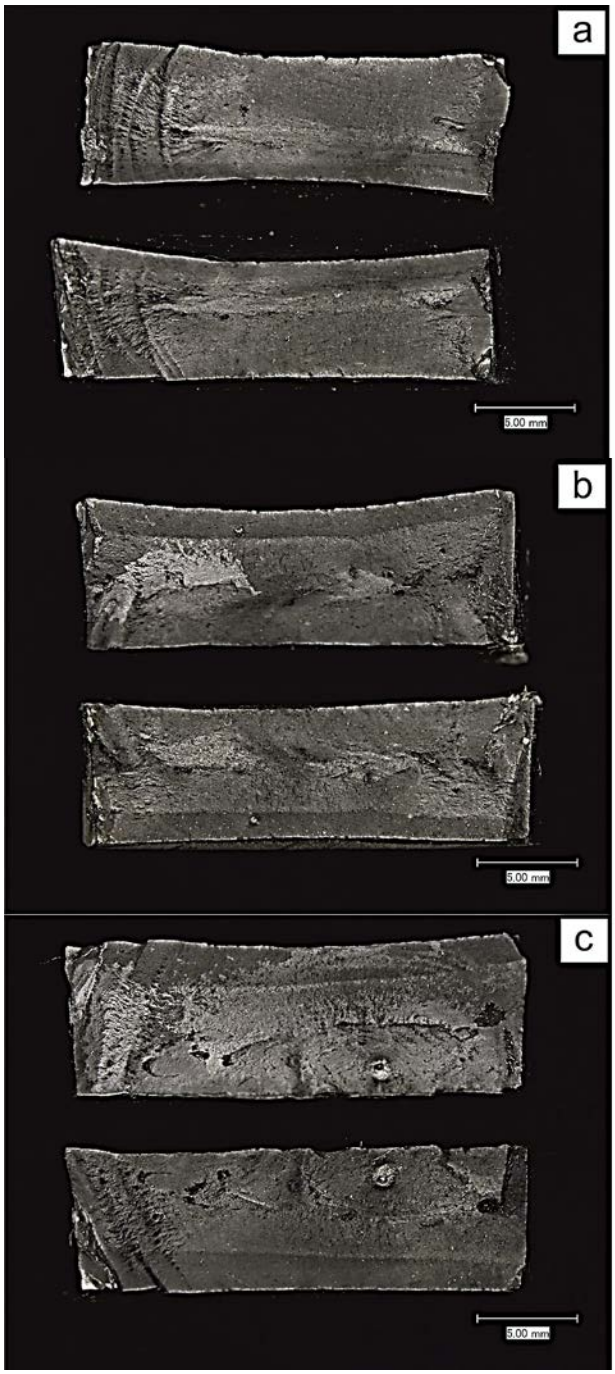

Figure 7. Optical macrographs of the fracture surface of the tensile test specimens; a) top, b) middle, c) bottom.

The fractured surfaces are presented in Figure 10 and 11. The base metal samples with high impact energy showed a fully ductile fracture, as shown in Figure 10(a). The fractured specimens of WMCL (Figure 14(b)) had two different fracture surfaces in a ductile and a brittle manner over part (~20%), and its impact value was relatively lower. The FL specimens gave the lowest values, and it had broader brittle zone about ~45%, as presented in Figure 14(c). The specimens between the WMCL and the FL possessed roughly 20% brittle zone (Figure 14(d).). They presented similar toughness values with the WMCL.

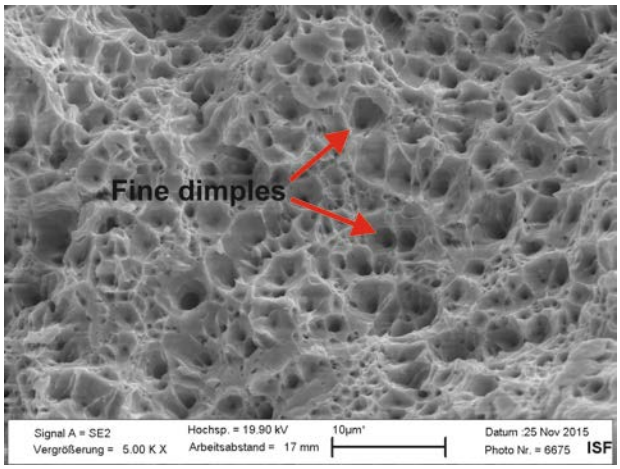

Figure 8. A selected SEM fractograph showing high magnification fracture surface of the tensile test specimen.

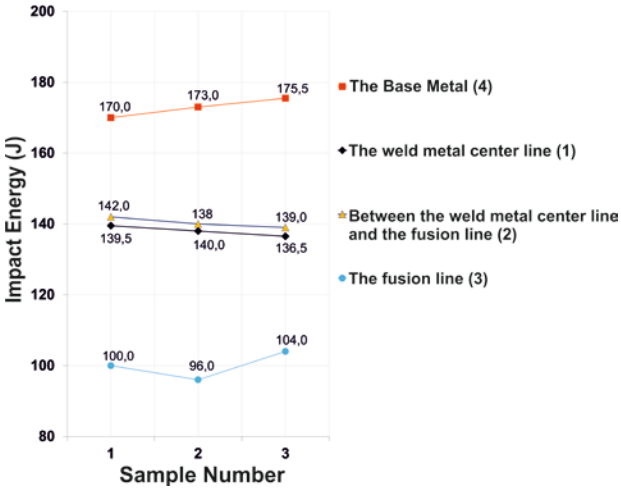

Figure 9. Absorbed energy values measured for the samples removed from the 25 mm thick plates at the room temperature.

3.5. Macrostructural investigation

The cross-sectional macrostructure of the SAW welded joint is presented in Figure 12. It is free from macro-level defects. The cross-section of SAW joint appears like hour-glass shape.

It comprises of columnar weld metal (FZ), HAZ (coarse-grained, fine-grain, intercritical), fusion boundary and base metal.

The weld metal composed of columnar dendritic grains, directed to the fusion line. Due to the fact that heat removal was supreme in the direction upright to the fusion line, the grains were in tendency to grow in that direction, ending up with in a columnar grain structure in the weld zone. Various sub-zones of the

HAZ experienced several top temperatures during the welding process, due to differences in distance from the WMCL. The grain size of the HAZ changed correspondingly. HAZ was subjected to the maximum temperature, which gave rise to grain coarsening.

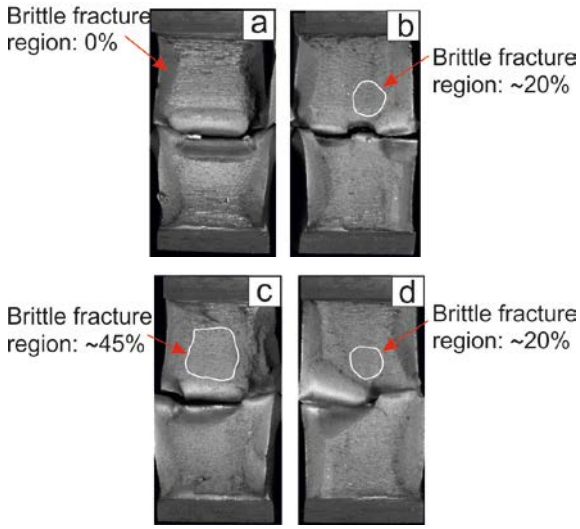

Figure 10. Optical macrographs of the fracture surface of impact toughness test samples; a) the base material, b) the WMCL, c) the FL, d) between the FL and the WMCL.

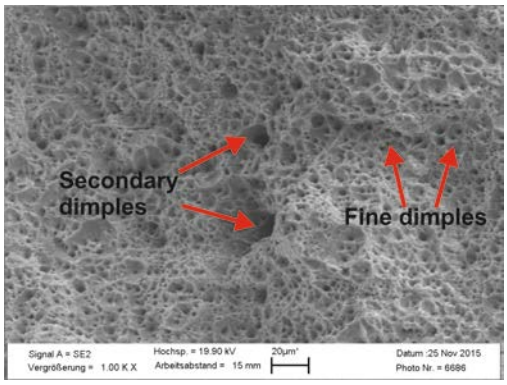

Figure 11. A selected SEM fractograph showing high magnification fracture surface of toughness test sample.

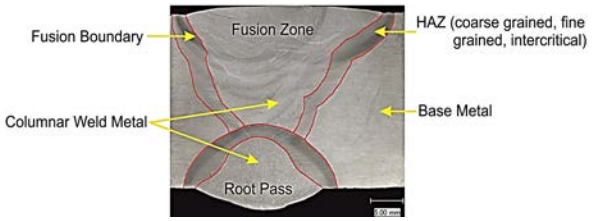

Figure 12. Microstructural zones of S960QL welded joint

3.6. Microstructural investigation

The microstructural examination on the samples of welded joint was carried out using LOM and with 500x, as shown in Figure 13. The weld metal had finer grain structure than the base metal. During the welding process, the joining was occurred by melting in the weld seam. Due to the melting in narrow zone, the rapid cooling conditions happened during the solidification of this zone, and the fine grain microstructure was obtained.

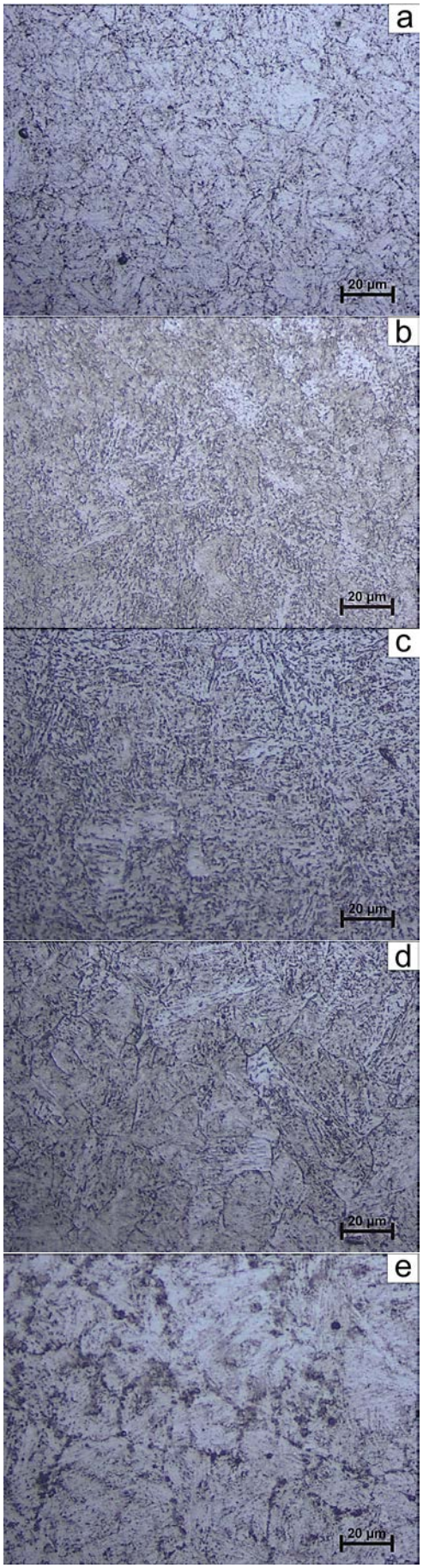

Figure 13. The microstructures of welded joint; a) the base metal, b) intersection of the root pass and the weld metal, c) between the FL and the WMCL, d) the WMCL, e) HAZ.

Investigating the interface of the FZ-HAZ and HAZ microstructures, it is seen that it had coarser grain structure than the base metal. The grain coarsening was occurred during the weld process because of the high heat input in HAZ. As mentioned above, alloy carbides dissolved because of the high temperature values occurred at HAZ and grain growth occurred easier.

4. Discussion and Conclusion

The aim of this research is to investigate the microstructural and mechanical properties of 25 mm thick S960QL HSLA steel welded by SAW, according to the selected parameters from ISO 26304:2011, instead of comparing the different welded samples. Following conclusions can be drawn:

Chemical analyses

The effect of experimental parameter changing on the distribution of alloying elements was not occurred since the analyses were carried out in a wide zone.

Hardness

Maximum hardness values were measured at the HAZ. It is consistent with the literature that the HAZ has hardenability. It was found that the obtained hardness distribution agrees with the literature. Hardness values of the WMCL were close to the base metal. At the row of the root pass from the center line to base metal, HAZ zone exhibited 350-448 HV0.3. Such hardness values for both multilayer passes and root pass reveal the potential risk of cracks in HAZ.

Tensile test

The tensile strength of the middle and the bottom flat type samples were higher than the minimum base metal values (>980 MPa) obtained by the producer and literature. The top flat type samples were relatively lower than the other flat samples. The elongations of the flat type samples were lower than the base metal. Previous studies support these results.

Notch impact toughness test

The base material gave the highest toughness values. The specimens between the FL and the WMCL achieved the best absorbed energies, following the base metal. The samples from the FL gave the lowest values. The similar result was obtained in a study on fracture behaviors of welded low carbon steels.

It is normal that the tensile strength and the toughness had low values, because of the deterioration of the grain structure, precipitates and the lost homogeneity.

Macrostructural investigation

The cross-section of SAW joint appears like hour-glass shape. The cross-sectional macrostructure comprises of several distinct regions, such as columnar weld metal (FZ), HAZ (coarse-grained, fine-grained, intercritical), fusion boundary and base metal.

Microstructural investigation

Due to the melting in narrow zone, the rapid cooling conditions happened during the solidification of weld metal and the fine grain microstructure was obtained. The grain coarsening was occurred during the weld process because of the high heat input in HAZ. The alloy carbides dissolved because of the high temperature values that occurred at HAZ and the grain growth was made easier.

Fracture surfaces

The LOM and SEM examination of fracture surfaces revealed that the modes of failure of the tensile test samples were ductile with acceptable plastic deformation. Fine and secondary dimples are signs of good tensile strength of this joint. The base metal specimens exhibited a completely ductile fracture surface and achieved a high absorbed energy. The fractured specimens of WMCL, the FL, and the zone of the FL-the WMCL had two different fracture surfaces in ductile and brittle manner, and the absorbed energies were slightly lower in these specimens.

During the welding process of S960QL steel, preheating, temperature between passes, heat input should be controlled strictly in keeping with the declared standards, in order to keep away from cold cracks and possible failures, and to achieve the required properties of welded structures. Inadequate heat input mostly influences hardness and the strength of these structures. Moreover, the hydrogen dissolution and residual stresses in the weld may result in cold cracks, while minimizing deformability and enhancing sensitiveness to embrittlement [29].

Acknowledgements

The author would like to thank colleagues at "Welding and Joining Institute-RWTH Aachen University". In addition, Konrad Willms, Johannes Schäfer and Rahul Sharma are very much appreciated and acknowledged for the valuable suggestions and technical support.

References

[1] V. R. Mattes. 1990. Microstructure and mechanical properties of HSLA-100 steel. M.Sc. Thesis, p. 3, Naval Postgraduate School, California, USA.

[2] S. Kumar, S.K. Nath. 2016. Effect of heat input on impact toughness in transition temperature region of weld CGHAZ of a HY 85 steel. Journal of Materials Processing Technology, 236, 216–224.

[3] B. K. Show, R. Veerababu, R. Balamuralikrishnan, G. Malakondaiah. 2010. Effect of vanadium and titanium modification on the microstructure and mechanical properties of a microalloyed HSLA steel. Materials Science and Engineering, A 527, 1595 – 1604.

[4] L. Wei, T.W. Nelson. 2012. Influence of heat input on post weld microstructure and mechanical properties of friction stir welded HSLA-65 steel. Materials Science and Engineering, A 556, 51 – 59.

[5] M. Opiela. 2010. Hydrogen embrittlement of welded joints for the heat-treatable XABO 960 steel heavy plates. Journal of Achievements in Materials and Manufacturing, 38, 41 – 48.

[6] A. J. Craven, K. He, L. A. J. Garvie, T. N. Baker. 2000. Complex Heterogeneous Precipitation in Titanium– Niobium Microalloyed Al-killed HSLA steels – I.(Ti,Nb)(C,N) particles. Acta Materialica 48, 3857 – 3868.

[7] American Society for Metals. 2001. High-Strength Low-Alloy Steels. Carbon and Alloy Steels. ASM, USA, pp.193.

[8] S. Nemat-Nasser, W. Guo. 2005. Thermomechanical response of HSLA-65 steel plates: experiments and modeling. Mechanics of Materials, 37, 379 – 405.

[9] L. Zhang, Th. Kannengiesser. 2014. Austenite grain growth and microstructure control in simulated heat affected zones of microalloyed HSLA steel. Materials Science and Engineering, A 613, 326 – 335.

[10] Q. Xue, D. Benson, M. A. Meyers, V. F. Nesterenko, E. A. Olevsky. 2003. Constitutive response of welded HSLA 100 steel. Materials Science and Engineering, A 354, 166 – 179.

[11] Q. Xue, D. Benson, M. A. Meyers, V. F. Nesterenko, E. A. Olevsky. 2003. Constitutive response of welded HSLA 100 steel. Materials Science and Engineering, A 354, 166 – 179.

[12] H. Jo Jun, K.B. Kang, C. G. Park. 2003. Effects of cooling rate and isothermal holding on the precipitation behavior during continuous casting of Nb–Ti bearing HSLA steels. Scripta Materialia, 49, 1081 – 1086.

[13] S. Sivaprasad, S. Tarafder, V. R. Ranganath, K. K. Ray. 2000. Effect of prestrain on fracture toughness of HSLA steels, Materials Science and Engineering, A 284, 195 – 201.

[14] J. J. S. Dilip, G. D. J. Ram, T. L. Starr, B. Stucker. 2017. Selective laser melting of HY-100 steel: Process parameters, microstructure and mechanical properties. Additive Manufacturing, 13, 49–60.

[15] V. Jablokov, D. M. Goto, D. A. Koss, J. B. McKirgan. 2001. Temperature, strain rate, stress state and the failure of HY-100 steel, , Materials Science and Engineering, A 302, 197–205.

[16] Beretta, S., Bernasconi, A., Carboni, M. 2009. Fatigue assessment of root failures in HSLA steel welded joints: A comparison among local approaches. International Journal of Fatigue, 31, 102–110.

[17] Gorni, A. A., Mei, P. R. 2004. Austenite transformation and age hardening of HSLA-80 and ULCB steels. Journal of Materials Processing Technology, 155–156, 1513–1518.

[18] Cwiek, J. 2005. Hydrogen assisted cracking of high-strength weldable steels in sea-water. Journal of Materials Processing Technology, 164–165, 1007–1013.

[19] Shen, S., Oguocha, I. N. A., Yannacopoulos, S. 2012. Effect of heat input on weld bead geometry of submerged arc welded ASTM A709 Grade 50 steel joints. Journal of Materials Processing Technology, 212, 286–294.

[20] Kiran, D. V., Basu, B., Dea, A. 2012. Influence of process variables on weld bead quality in two wire tandem submerged arc welding of HSLA steel. Journal of Materials Processing Technology, 212, 2041–2050.

[21] Chandel, R. S., Seow, H. P., Cheong, F. L. 1997. Effect of increasing deposition rate on the bead geometry of submerged arc welds. Journal of Materials Processing Technology, 72, 124–128.

[22] Fatehi, A., Calvo, J., Elwazri, A. M., Yue, S. 2010. Strengthening of HSLA steels by cool deformation. Materials Science and Engineering, A 527, 4233–4240.

[23] Jun, H. J., Kang, K. B., Park, C. G. 2003. Effects of cooling rate and isothermal holding on the precipitation behavior during continuous casting of Nb–Ti bearing HSLA steels. Scripta Materialia, 49, 1081–1086.

[24] Garašić, I., Ćorić, A., Kožuh, Z., Samardžić, I. 2010. Occurrence of cold cracks in welding of high-strength S960QL steel. Technical Gazette 17, 3, 327-335.

[25] Porter, D. A. 2015. Weldable High-Strength Steels: Challenges and Engineering Applications. IIW International Conference, 2-3 July, Helsinki, 1-14.

[26] Ada, H. 2006. Weldability of Pipes Produced for Crude Oil and Natural Gas Pipelines with The Method of Submerged and Spiral Arc Welding and Researching Their Mechanical Properties, M.Sc. Thesis, p. 145, Gazi University, Ankara.

[27] Kou, S. 2003. Welding Metallurgy. John Wiley & Sons Inc. Publication. New Jersey, USA, 405 pp.

[28] Kim J. H., Oh, Y. J., Hwang, II S., Kim D. J., Kim J. T. 2001. Fracture behavior of heat-affected zone in low alloy steels. Journal of Nuclear Materials, 299, 132-139.

[29] Dunđer, M., Vuherer, T., Samardžić I., 2014. Weldability of microalloyed high strength steels TStE 420 and S960QL. Metalurgija 53, 3, 335-338.